Electro-thermo-dynamic performance of a microgripping system

Zeman, Marco; Bordatchev, Evgueni V.; Knopf, George K.

Publisher's version / Version de l'éditeur:
https://doi.org/10.1109/ICMA.2005.1626842
Mechatronics and Automation, 2005 IEEE International Conference, pp. 1848-1853, 2005

Electro-Thermo-Dynamic Performance of a Microgripping System

Evgueni V. Bordatchev
Integrated Manufacturing Technologies Institute
National Research Council of Canada
London, Ontario, Canada N6G 4X8
evgueni.bordatchev@nrc.gc.ca

Marco Zeman, George K. Knopf
Department of Mechanical & Materials Engineering
The University of Western Ontario
London, Ontario, Canada N6A 5B9
mjzeman2@uwo.ca, gknopf@engga.uwo.ca

Abstract - **Microgripping systems incorporate miniature end grasping tools to manipulate micro-sized objects such as tiny mechanical parts, electrical components, biological cells, and bacterium. A thorough understanding of the system's dynamic behaviour, including the gripper force and tip displacement, is essential for successfully handling these micro-objects. In this paper, the electro-thermo-dynamic performance characteristics of a proposed microgripper are described. The system has a monolithic design which consists of a combination of an in-plane electro-thermally driven microactuator and a compliant mechanism. The kinematics of the microgripper is introduced and several prototypes are fabricated from 25μm thick nickel foil. The dynamic and electro-thermal characteristics of the system are analyzed with respect to step responses, actuation/tweezing displacements, applied current/power, actual resistance and overall average temperature. Experiments demonstrate that the fabricated microgripper prototype with design parameters of $\alpha_0 = 30°$, $\beta_0 = 40°$, $h_0 = 0$μm, and $l_0 = 1.2$mm achieves tweezing displacement of 11.84μm (tweezing gap of 23.68μm) for an applied voltage and current of 1.41V and 0.15A, respectively. This experimental observation agrees with the predicted displacements from the kinematic model of 11.66μm. These preliminary results lay a foundation for developing micro grasping end-effectors for microrobotic and microassembly applications.**

Index Terms - **Microgripper, compliant mechanism, microactuator, kinematic simulation, electro-thermo-dynamic behaviour.**

I. Introduction

Microgrippers and microtweezers have been used as miniature end-effectors in a variety of applications including mechanical micro-assembly, micro-robotics and biological cell manipulation. A diversity of microgripper designs is necessary to carefully grasp and handle these fragile micro-objects with geometric dimensions below one hundred micrometers. Consequently, the microgripper is a complex micro-electro-mechanical system, the performance of which depends upon the material properties, method of actuation, part geometry and the kinematic behaviour of the design.

These micro-electrical-mechanical systems (MEMS) require a sophisticated method of actuation which is based on fundamental material properties in order to achieve a gripping motion. The most common microactuation methods are based on electrostatic, piezoelectric, electro-thermal, and shape memory alloy (SMA) effects. Typical electrostatic actuators require very high voltages, as demonstrated by the electrostatic gripper created by Lee et al. [1] requiring 250V to function properly. Even with high voltages in the range of 80V, only relatively small displacements of up to 20μmwere observed [2]. Similarly, piezoelectric actuators also require high voltages. The microgripper created by Menciassi et al. [3] required 150V to achieve a tip displacement of 395μm. Kohl et al. [4-5] created an SMA microgripping system which relied on one-way shape memory and therefore required two separate mechanisms of actuation for closing and opening of the gripping jaws. The device achieved a maximum stroke of 300μm with applied power of 80mW. The actuation components in this design reach a maximum temperature of 59°C. A larger 1.7cm long SMA microgripper introduced by Roch et al. [6] could achieve a tip displacement of 250μm with a 1V and 0.9A source.

This paper presents a new microgripper design, its kinematics, and also the experimental performance on several fabricated microgrippers. Two methods of testing are explored, constant voltage and current controls. By better understanding the effects of the testing methods on the microgripper, proper control and predictable results are achieved. Several electro-thermo-dynamic characteristics including applied current/ power, averaged temperature, actual resistance, and gripping gap, are studied. In addition, the dynamics of the proposed microgripper is studied using a step response function and then was compared with the simulation results obtained from the kinematic model.

II. Design of Microgripping System

The design of the microgripper based on a compliant mechanism attached to an in-plane microactuator is shown in Fig. 1. The microgripper is a monolithic 2-D structure where the microactuator and the compliant mechanism are linked using compliant flexible hinges. The microactuator is based on a multi-cascaded approach [7-9] and has seven actuation units. The design consists of a pair of identical, vertically oriented, cascaded actuation structures. Each actuation structure has seven actuation units connected serially in order to magnify the output vertical displacements. The actuation unit is composed of two actuation beams and one constraining beam. The actuation beam is a V-shaped bent (chevron type) beam. The pair of vertically parallel actuation structures are linked together by a horizontal motion platform. Also, the

actuation structure has a fixed electrical pad, or anchor, to apply power to the circuit.

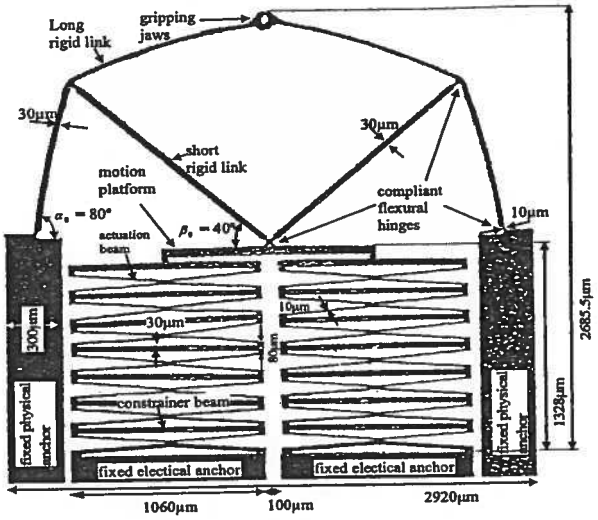

Fig. 1. Photograph of the basic microgripping system.

The gripping mechanism represented by the compliant mechanism consists of a pair of gripping arms which represents a mirror image of each other and reflected about the vertical center of the microgripper. Each gripping arm has short and long rigid links, three compliant flexural hinges, and a gripping jaw. One end of the short rigid link is connected to the motion platform of the microactuator and the other connected to the long rigid link. The long rigid link ended with a gripping jaw, is connected to a physical anchor. All joints between the links and microactuator are joined by the compliant flexural hinges with a width of 10 microns.

On application of a voltage across the fixed electrical anchors of the microactuator to form a closed loop, the output displacement is generated from the summation of all seven actuation units in one cascaded structure. The direction of motion of the actuation beams can be outward (stretching mode) or inward (shrinking mode), depending on whether the actuation beams are under expansion or contraction. The symmetric monolithic structure was chosen to provide symmetrical distribution of voltage, temperature and displacements along each vertical cascaded structure.

While current flows through the microactuator, thermal expansion causes an in-plane displacement pushing upward consequently pushing the rigid links outward, opening the gripping jaws. Once the electrical current is removed, the microactuator cools and retracts returning the gripping jaws to their originally closed position. The compliant mechanism does not provide a closed electrical path, therefore current will not flow through the center hinge and the compliant mechanism.

Microgrippers studied in this report were fabricated from a 25μm thick pure nickel foil using the laser microfabrication technology [7,9,10]. The parameters of the laser-material removal process, such as laser power, pulse repetition rate, working distance, and feed rate, were optimized in order to achieve accuracy and precision of the fabricated prototype within +/– 1μm.

III. KINEMATICS OF MICROGRIPPING SYSTEM

A functional relationship between the in-plane linear actuation motions $h(t)$ and tweezing motions $x(t)$, must be described in order to understand the relation of all parameters. Fig. 2 shows the kinematics of the microgripping system. As a dynamic system, the microgripper has one input (h) provided by the microactuator and one output (x). The vertical motions of the gripping jaw are not described in this paper. The compliant mechanism has two functions. It geometrically transforms input vertical actuation motions into output horizontal tweezing motions and it amplifies tweezing motions. By providing the kinematics of the microgripping system, the distance between gripper jaws can be predicted with respect to a given actuation of the linear microactuator.

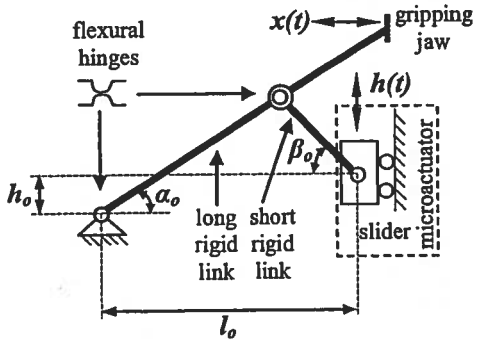

Fig. 2. Kinematics of the microgripping system.

The kinematics can be represented by the transform coefficient, K, which is defined by several geometric parameters. These parameters include h_0, the initial vertical offset; α_0, the angle of the long rigid link; β_0, the angle of the short rigid link; and l_0, the distance between the one end of the long rigid link and the end of the short rigid link attached to the moving platform of the microactuator. In general, the tweezing motion, x, can be expressed as:

$$x = K\,h, \text{ where } K = K(h_0, \alpha_0, \beta_0, \ell_0) \qquad (1)$$

The detailed kinematic model and comprehensive simulation of the kinematics (1) can be found in [11].

Fig. 3 illustrates the simulation results of the microgripper's kinematic performance given h_0 = 0μm, α_0 = 30°, β_0 = {10°, 20° … 80°}, and l_0= 1.2mm. The simulation results show that $K(h_0, \alpha_0, \beta_0, l_0)$ can be linearly approximated as:

$$K = \tan(x/h) \qquad (2)$$

and calculated as K = 0.585 for the gripping mechanism with

the design parameters of $\alpha_0 = 30°$, $\beta_0 = 40°$, $h_0 = 0\mu m$, and $l_0 =$ 1.2mm. The results of this simulation and simplified kinematic model (2) are used in Section V for comparative study on experimental results.

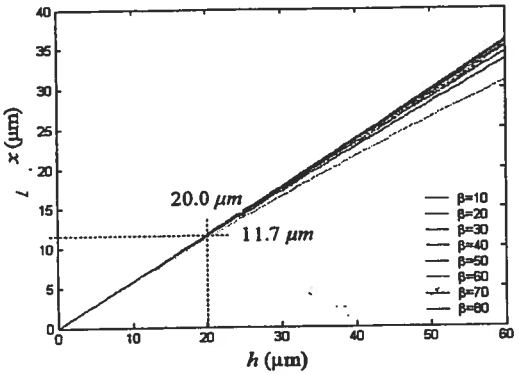

Fig. 3. Relationship between the in-plane actuation (h) and tweezing movement (x) based on simulation of the microgripper's kinematics.

IV. Experimental Setup and Procedure

The experimental setup for evaluating the performance characteristics of the fabricated microgripper is shown in Fig. 4. The setup consists of a power supply (Agilent A3631A), 1Ω power resistor, digital oscilloscope (LeCroy WaveRunner, LT354), optical microscope (Olympus, SZX12) with a CCD camera under Visual Gauge ™ software control, and desktop computer. The microgripper is mounted on a small piece of glass glued to a plastic container and it was wired to a standard socket for electrical connections. Two channels of the oscilloscope are connected to the circuit: one to measure the applied voltage across the microgripper, and the other to measure the applied current across the power resistor. A standard multimeter was used to measure the electrical resistance and found to be 3.2 Ω for the seven actuation unit microactuator. The total resistance of the connecting wires was 0.4 Ω.

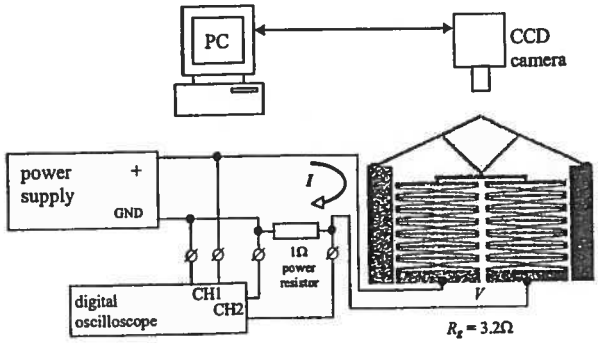

Fig. 4. Experimental setup for testing microgripper performance.

Several microgripper prototypes were designed and fabricated with design parameters $h_0 = 0\mu m$, $\alpha_0 = 30°$, and $l_0 =$ 1.2mm, $\beta_0 = \{10°, 20°, \ldots 80°\}$, and identical actuators with seven actuation units.

The performance evaluation involved the following steps. By switching the power supply, voltage and current are applied to the microgripper as a step input. Simultaneously, applied voltage and current are recorded by the digital oscilloscope, and the planar displacements of the motion platform of the microactuator and tweezing motions of the compliant mechanism are captured by a CCD camera through the optical microscope for further analysis. The experimental setup enables two testing methods to be performed: *(i)* constant voltage control (CVC), and *(ii)* constant current control (CCC). Fig. 5 shows typical electrical step response characteristics under CVC and CCC testing. Fig. 6 illustrates the microgripper's actual performance where the total gap between gripping jaws is double the tweezing motion, x. The tweezing distance is always measured for a single gripper pad.

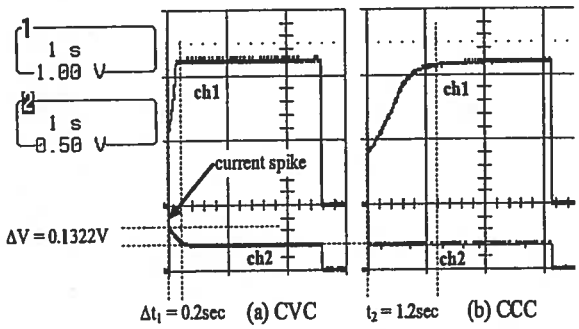

Fig.5. Typical electrical step response characteristics for (a) constant voltage control and (b) constant current control.

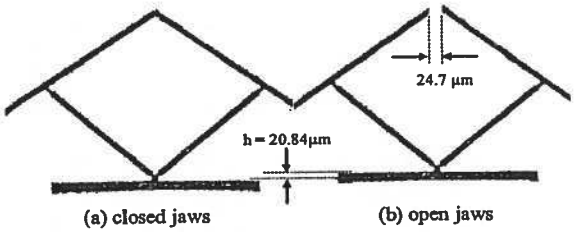

Fig. 6. Actual dynamic performance under applied current of 0.15 A.

The purpose of testing the microgripper was to obtain the electro-thermo-dynamic performance characteristics and to compare them with the results from kinematic simulation. Several electro-thermo-dynamic characteristics are studied: (i) step response under constant voltage control; (ii) step response under constant current control; (iii) actuation displacements vs. applied current and power; and (iv) calculated temperature vs. applied current, power, and microgripper resistance.

V. Experimental Results and Analysis

A. Dynamic performance

The dynamic performance of the fabricated microgripper

was studied based on step response characteristics with respect to actuation (input) and tweezing (output) motions. Fig. 7 shows the step response under CVC and CCC testing with an applied voltage of 1.41V across the microgripper and a current of 0.15A, respectively. During these tests the actual actuation motions, $h(t)$, and tweezing motions, $x(t)$, were measured, and the expected tweezing motions, $\hat{x}(t)$, and dynamic error, $\Delta x(t)$, were calculated as:

$$\hat{x}(t) = K\, h(t) \tag{3}$$

$$\Delta x(t) = x(t) - \hat{x}(t) \tag{4}$$

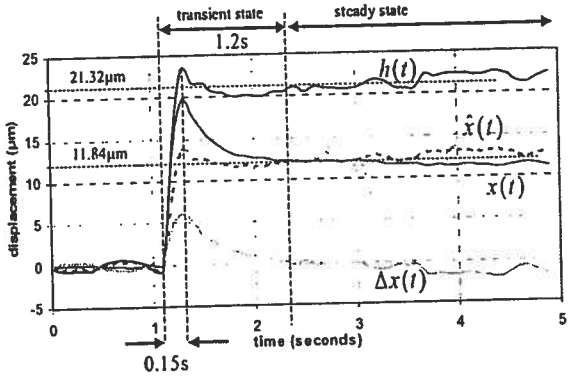

(a) constant voltage control under applied 1.41V.

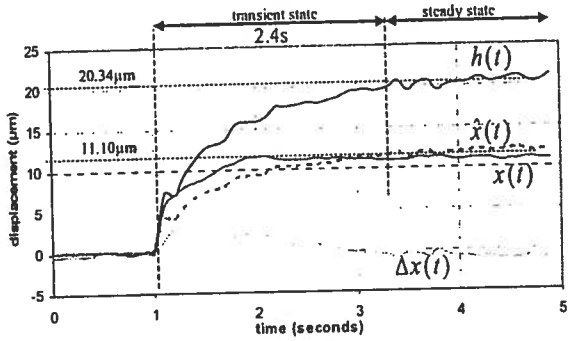

(b) constant current control under applied 0.15A.

Fig. 7. Step responses of the microgripper.

During the CVC test, Fig. 7(a), $x(t)$ reaches a peek at 19.67μm and then drops to 11.84μm at steady state after the transient stage of 1.2s. This is very close to the expected steady state tweezing distance of 11.66μm. Therefore, the microgripper performance has an overshoot of 7.83μm. The actuation motions, $h(t)$, are smoother, where as $h(t)$ peeks at 23.36μm and drops by only 2.04μm to steady state. The difference between the transient states of $h(t)$ and $x(t)$ seems to be due to the delay between the thermo-dynamic expansion of the microactuator and mechanical response of the gripping mechanism. The actuation beams expand due to the heating effect of the current flow and consequently causing softening of the material. This softening reduces the stiffness of the entire microactuator reducing the force that pushes the compliant mechanism upward. Eventually, the force pushing downward, due to the stiffness of the compliant gripping mechanism, matches the upward force of the thermally expanded microgripper during steady state (static performance). Steady state occurs when the natural convection of the heat from the actuation beams becomes constant, as shown when the dynamic error approaches zero at steady state (see Fig. 7a).

Furthermore, a current spike occurs for the CVC test after 0.15 seconds, whereas the peek in the electrical response of the current spike seen in Fig. 5a rises instantly after the power supply is turned on. There is a delay in the current spike of the displacement response in comparison to the electrical response in achieving steady state. This delay is a result of the difference in the heating rate and the thermal response of the microgripper system induced by the current flowing through the microactuator. Since a current spike occurs only in the CVC test, the heat rate increase is quicker, causing thermal expansion to occur faster allowing the microgripper to reach steady state in half the time of the CCC tests.

The step response for constant current control (CCC) test is given in Fig. 7b. The results show no overshoot. By using either the CVC or CCC tests, the same steady state tweezing displacements, 11.84μm and 11.10μm, respectively, were achieved. These values closely match those presented in Fig 3. However, it is necessary to note that the setting time for the CCC test is two times longer than for the CVC test; that is, 2.4s vs. 1.2s.

Fig. 8 illustrates the overall performance of the microgripping system in terms of actuation and tweezing displacements with respect to the applied current and power. During the experiment, the applied current was increased within a range of {0.03A, 0.05A... 0.17A}.

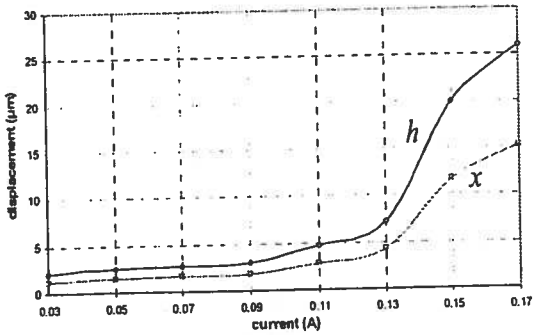

(a) actuation/tweezing displacements vs. applied current

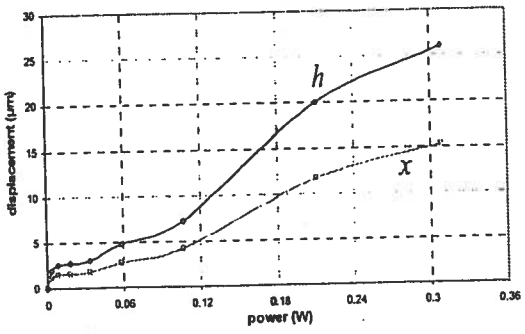

(b) actuation/tweezing displacements vs. applied power

Fig. 8. Overall performance of the microgripping system.

The tweezing motions exponentially increase along with linear increase in the applied current for which maximum tweezing displacement of 12.58μm was recorded for an applied current of 0.17A. These relationships characterize the dynamic performance of the microgripping system and allow the user to choose optimal control parameters to obtain and sustain desired tweezing displacements and forces in practical applications. Based on the above results, the CCC testing methodology was chosen for evaluation of the electro-thermal characteristics.

B. *Electro-Thermal Characteristics*

The objective of the analysis described below is to investigate the variations in resistance and the overall average temperature of the microgripper due to the thermo-electric effect during actuation. Initially, the current-voltage characteristics were obtained and the actual resistance was calculated using classical Ohm's law (Fig. 9). By increasing the applied current within a range of {0.02A, 0.03A,...0.17A}, the applied voltage was measured and resistance of the microgripper was calculated. Results show that as soon as the current was applied and the heat generated, the microgripper changed its resistance substantially from 3.2Ω, for 0.064V and 0.02A, to 7.84Ω, for 1.33V and 0.17A. Fig. 9 shows that resistance and voltage increase exponentially over a constant increase in current.

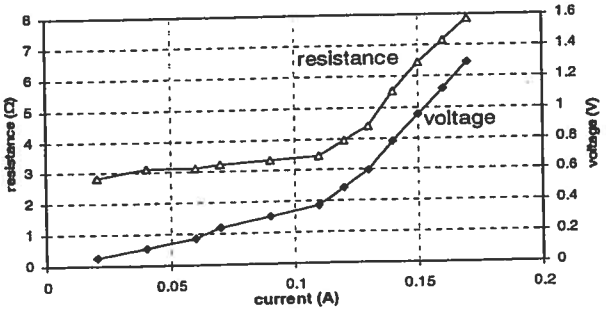

Fig. 9. Resistance & voltage as a function of current.

The microgripper has a monolithic structure fabricated from pure nickel foil and therefore it exhibits a change in resistance when undergoing a change in temperature causing change of the physical-mechanical properties and the thermal-expansion coefficient of the nickel [13, 14]. Since the cross-sectional area of the actuation beams in the microactuator is only 250μm^2, this creates a bottleneck for the current flow, therefore a substantial increase in temperature and resistance is expected.

At room temperature ($T_{initial}$ = 20°C), a seven unit microactuator has a resistance of 3.2Ω. The final resistance of the microgripper, R_{final}, at higher temperatures during testing, can be determined using classic formula:

$$R_{final} = R_{initial}[1+\alpha(T_{final} - T_{initial})] \quad (5)$$

where α is the thermal coefficient of resistance of α = 6600ppm/°C pure nickel [15].

Data from Fig. 9 were used to calculate the overall average temperature of the microgripper, T_{final}, at any applied current. Fig. 10 shows calculated characteristics of the average temperature over actual resistance of the microgripper, applied current, and power. As expected, the resistance of the microgripper increases linearly with respect to temperature. The microgripper reaches a maximum overall temperature of 288°C for an applied current of 0.17A.

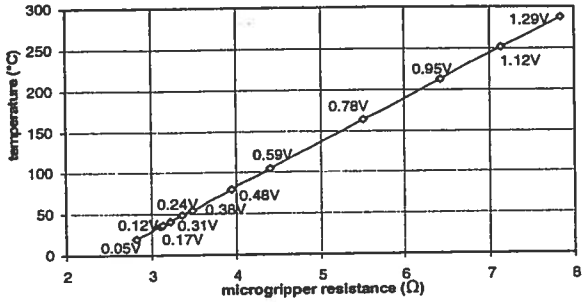

(a) temperature vs. resistance.

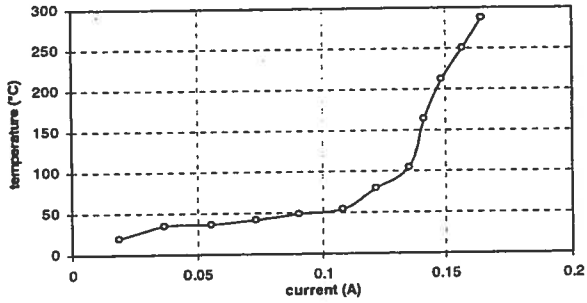

(b) temperature vs. applied current.

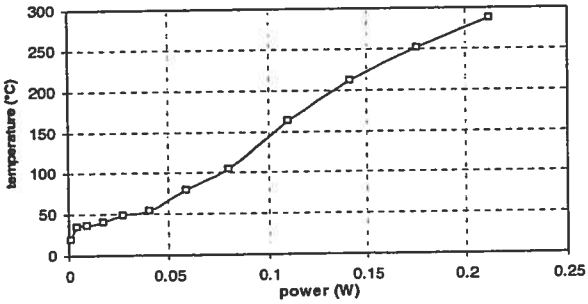

(c) temperature vs. applied power.

Fig. 10. Electro-thermal characteristics of the microactuator.

VI. Summary and Conclusions

This paper presents a systematic study of the electro-thermo-dynamic behaviour of a proposed microgripping system. The microgripper consisted of a monolithic 2-D structure with rigid links that joined the microactuator shell

and the compliant mechanism using flexible hinges. The microgripper was fabricated from a 25μm thick pure nickel foil using the laser microfabrication technology and its performance was experimentally evaluated using constant voltage and constant current control. The dynamic and electro-thermal characteristics of the microgripping system were analyzed with respect to step responses, actuation/tweezing displacements, applied current/power, actual resistance and overall average temperature. For a microgripper prototype with design parameters of $\alpha_0 = 30°$, $\beta_0 = 40°$, $h_0 = 0\mu m$, and $l_0 = 1.2mm$, the tweezing displacements of 11.84μm (with a tweezing gap of 23.68μm) were obtained under an applied current of 0.15A. This observation agrees well with the predicted displacement of 11.66μm derived from the kinematics simulation of the system.

The following conclusions can be drawn from these preliminary studies:

1. The microgripper being a complex actuation system, is both reliable and repeatable, and also capable of generating accurate tweezing motions.
2. The microgripper delivers smooth tweezing motions under the constant current control (CCC) operation without an overshoot or destructive current/voltage spikes.
3. The constant voltage control (CVC) operation is not suitable for practical tweezing applications because of significant overshoot observed in the gripper movement. For example, an overshoot of 8.16μm was observed for an applied voltage of 1.41V, a result that could seriously damage a microsample.
4. The kinematic model can reliably predict the dynamic performance of the proposed microgripper.
5. The developed microgripping system exhibits a complex nonlinear electro-thermal characteristic. It significantly changed resistance from 3.2Ω, for applied 0.064V and 0.02A, to 7.84Ω, for applied 1.33V and 0.17A, attaining an overall average temperature of 288°C.
6. The microgripper can be used for handling and manipulation of miniature mechanical components and biological cells as long as the application requirements fall within the system specifications.

ACKNOWLEDGMENT

This paper is the result of the collaboration between IMTI-NRC and The University of Western Ontario, London Ontario, Canada. The authors thank Mr. Mahmud-Ul Islam, Director, Production Technology Research, NRC-IMTI, and Dr. Suwas Nikumb, Group Leader, Precision Fabrication Processes, NRC-IMTI, for their continued support in this work. The authors also appreciate the assistance of Mr. Hugo Reshef for his help in performing the laser fabrication. This study was partially supported by NSERC Discovery Grant R3440A01.

REFERENCES

[1] S. E. Lee, K. C. Lee, and S. S. Lee, "Fabrication of an Electrothermally Actuated Electrostatic Microgripper," *International Journal of Nonlinear Sciences and Numerical Simulation*, 2002, pp. 789-793.

[2] B. E Volland., H. Heerlein, and I. W. Rangelow, "Electrostatically driven microgripper," in *Microelectronic Engineering*, Vol. 61-62, 2002, pp. 1015-1023.

[3] A. Menciassi, A. Eisinberg, M. Mazzoni, and P. Dario, "A Sensorized μElectro Discharge Machined Superelastic Alloy Microgripper for Micromanipulation: simulation and characterization," *Proceedings of the 2002 IEEE/RSJ Intl. Conference of Intelligent Robots and Systems*, October 2002, Lausanne, Switzerland, pp. 1591-1595.

[4] M. Kohl, B. Krevet, and E. Just, "SMA Microgripper System," *Sensors and Actuators: A*, Vol. 97-98, 2002, pp. 646-652.

[5] M. Kohl, E. Just, W. Pfleging, and S. Miyazaki, "SMA Microgripper with Integrated Antagonism," *Sensors and Actuators: A*, Vol. 83, 2000, pp. 208-213.

[6] I. Roch, Ph. Bidaud, D. Collard, and L. Buchaillot, "Fabrication and Characterization of an SU-8 Gripper Actuated by Shape Memory Alloy Thin Film," in *Journal of Micromechanics and Microengineering 13*, 2003, pp. 330-336.

[7] E. V. Bordatchev and S.K. Nikumb, "Electro-Thermally Driven Microgrippers for MEMS Applications," accepted to be published in *Journal of Microlithography, Microfabrication, and Microsystems*, October 2004, scheduled to be published in July-September issue 2005, paper 04114R, in press.

[8] C.-P. Hsu, W.-C. Tai, and W. Hsu, "Design and Analysis of an Electro-Thermally Driven Long-Stretch Micro Drive with Cascaded Structure," *Proceedings of the ASME International Mechanical Engineering Congress*, November 17-22, 2002, New Orleans, Louisiana, USA, pp. 235 – 240.

[9] E. V. Bordatchev, S.K. Nikumb, and W. Hsu, Fabrication of Long-Stretch Microdrive for MEMS applications by Ultra Precision Laser Micromachining, *Proceedings of 2002 NRC-NSC Canada-Taiwan Joint Workshop on Advanced Manufacturing Technologies*, Editors: L. Wang, E. Bordatchev, S.-M. Tsay, and S. Lang, 23-24 September 2002, London, Ontario, Canada, pp. 243-252.

[10] E.V. Bordatchev, S.K. Nikumb, and W. Hsu, "Laser micromachining of the miniature functional mechanisms," in *Photonics North 2004: Photonic Applications in Astronomy, Biomedicine, Imaging, Materials Processing, and Education, Proceedings of SPIE*, Vol. 5578 (SPIE, Bellingham, WA, 2004), paper # 5578D-77, pp. 579-588.

[11] M. Zeman, E.V. Bordatchev, and G.K. Knopf, "Design, Kinematic Modeling & Testing of a Microgripper for Micromanipulation Applications," to be submitted in the *Journal of Micromechanics and Microengineering, Institute of Physics*.

[12] Y. Lai, E.V. Bordatchev, S.K. Nikumb, and W. Hsu, "Characterization of Static Performance of In-plane Electro-Thermally Driven Linear Microactuators," submitted to *Journal of Micromechanics and Microengineering, Institute of Physics*, in January 2005, unpublished.

[13] T A. Faisst, "Determination of the Critical Exponent of the Linear Thermal Expansion Coefficient of Nickel by Neutron Diffraction," *J. Phys.: Condens. Matter*, Vol. 1, 1989, pp. 5805-5810.

[14] T G. Kollie, "Measurement of the thermal-expansion coefficient of nickel from 300 to 1000 K and determination of the power-law constants near the curie temperature," *Physical Review: B*, Vol. 16, No. 11, 1977, pp. 4872-4882.

[15] R.B. Ross, *Metallic Materials Specification Handbook*, Fourth Edition, Chapman & Hall, New York, 1994, p.229.